Coupled hydro-mechanical analyses of a multi-tier geosynthetic-reinforced soil slope subject to rainfall infiltration

Kuo-Hsin Yang
National Taiwan University, Taiwan

Joseph Ng'ang'a Thuo
Dedan Kimathi Universtiy of Technology, Kenya

Jyun-Wei Chen
National Taiwan University of Science and Technology, Taiwan

Chia-Nan Liu
National Chi-Nan University, Taiwan

ABSTRACT: This paper presents a case study and numerical investigation of a failure of a geosynthetic-reinforced soil slope with marginal backfill subject to rainfall infiltration. The investigated slope is a 26 m high, 4 tier geogrid-reinforced slope constructed for stabilizing the existing highly weathered and fractured sandstone road embankment. Contrary to the backfill recommendations in design guidelines, locally available low plasticity silty clay (CL-ML) with over 60% of fines, was used as backfill in the reinforced zone. The GRS slope first experienced excessive deformation after seasons of typhoon and heavy rainfall from 2010-2013. The measured settlement and horizontal deflection at slope crest were 140 and 80 cm from June to December 2012. Although an immediate remedial action had been taken, the slope final collapse was caused by two sequential typhoon events with total accumulated rainfall of over 600 mm in August 2013. The failure mode was identified as the compound failure which had the failure surface partially cut through the reinforced zone at the lowest tier of the slope and partially passed along the interface between retained weathered layer and intact rock. Using recorded rainfall, site geology, and measured soil and reinforcement parameters, a series of coupled hydro-mechanical finite element analyses based on the framework of unsaturated soil mechanics were performed to examine the failure mechanism and causes contributing to the failure. The numerical results indicate the slope failure was attributed to positive porewater pressure accumulation within reinforced zones. Lessons learned from this case history are discussed.

Keywords: Geosynthetics, Reinforced slope; Marginal backfill; Rainfall infiltration; Failure, Hydro-mechanical analysis

1 INTRODUCTION

To stabilize unstable cut slopes, geosynthetic reinforced soil (GRS) walls and slopes have been preferred due to increased economic advantages and reported successful performances. However, design guidelines (AASHTO, 2002; Elias et al., 2001) limit the use of fine-grained soils as backfill material within the reinforced zone. Nevertheless, to minimize transportation cost and environmental impact associated with the disposal of the excavated soil, locally available soils with relatively low hydraulic conductivity (usually referred to as marginal fills) have been used as alternative backfills where granular backfill is not readily available (Hedayati and Hossain, 2015; Thuo et al., 2015; Zornberg and Mitchell, 1994).

Under unsaturated soil conditions, marginal backfills have been reported to perform satisfactorily due to presence of matric suction (Leshchinsky, 2009; Vahedifard et al., 2016). The presence of suction can increase soil effective stress, and thus enhance performance and stability of reinforced soil structures through increasing soil stiffness and shear strength , increasing soil-reinforcement interface strength (Vahedifard et al., 2016; Zornberg and Mitchell, 1994) and reducing mobilized reinforcement load (Vahedifard et al., 2016).

However, upon wetting by infiltrating ground water or rainfall, low draining capacity of fine soils has also been reported to compromise performance (excessive deformation) and even cause failure of GRS structures owing to the development of positive porewater pressure (Koerner and koerner, 2012; Zornberg and Mitchell, 1994). Nevertheless, many studies have demonstrated that marginal backfill can be used as alternative backfill provided adequate drainage is provided (Christopher and Stulgis, 2005; Mitchell and Zornberg, 1995; Portelinha et al., 2013).

Conventionally, GRS walls are designed using earth pressure theory while slopes are designed using limit equilibrium methods. Among other limitations, earth pressure theory assumes sufficient and adequate drainage is provided and does not consider the effect of seepage forces to wall stability (Ku et al., 2009). On the other hand, although the effect of pore water pressure to the stability of the reinforced slope can be factored during design (using limit equilibrium analysis), the location of the phreatic surface within to be constructed slope is usually not known and is assumed without clear guideline in most cases. Furthermore, both earth pressure and limit equilibrium methods do not evaluate the effect of pore water pressure to the mechanical behavior (deformation) of the wall/slope structure or backfill soil (Ku et al., 2009).

Assessing the hydrological response of unsaturated slopes subject to rainfall infiltration is critical and challenging, especially when determining the variation of PWP within slopes. To more accurately describe the physical responses (i.e., variation of soil moisture, matric suction, effective stress, soil shear strength, and slope stability) of unsaturated soil subject to infiltration, coupled and uncoupled hydro-mechanical analyses based on the framework of unsaturated soil mechanics have recently been performed (Oh and Lu, 2015; Qi and Vanapalli, 2015). Coupled analysis has been found to produce a reasonably well defined wetting front (Hamdhan and Schweiger, 2013; Qi and Vanapalli, 2015) and hence leads to a more accurate assessment of slope stability under infiltration conditions and demonstrates a better physical representation of water flow and stress variation within unsaturated soils (Yang et al., 2017). Numerous studies have been conducted on the performance of reinforced soil walls and slopes subject to rainfal infiltration. However, there is limited studies on the effect of pore water variation caused by rainfall infitration to mechanical performance of GRS walls or slopes with marginal backfills.

This paper presents a case study of a 26 m high, 4 tier geogrid-reinforced soil slope constructed for traffic demands in mountainous area of Taichung, Taiwan. Contrary to the backfill recommendations in design guidelines, low plasticity silty clay (CL) with over 60% of fines was used as backfill in the reinforced zone. The GRS slope first experienced excessive deformation after seasons of typhoon and heavy rainfall from 2010-2012. The measured settlement and horizontal deflection at wall crest were 140 and 80 cm from June to December 2012. Although an immediate remediation had been conducted for the wall excessive deformation, finally this wall collapsed after two sequential typhoon events with total accumulated rainfall over 600 mm in August 2013. A series of coupled hydro-mechanical finite element analyses were performed based on the framework of unsaturated soil mechanics. Field and laboratory test data obtained from site investigations were applied as input material properties and initial conditions in the numerical model. The objectives of this paper are as follows: (1) to investigate the failure and deformation mechanisms of this GRS slope; (2) to suggest potential remedial measures to mitigate the catastrophic damage and failure caused by heavy rainfall; (3) to propose design approach and construction implication for GRS structures with marginal backfill. This study demonstrated the suitability and applicability of hydro-mechanical analysis to predict the failure and deformation of unsaturated reinforced structures by using the selected case study. The causes of slope deformation and failure are discussed, remediation measures based on the revealed failure and deformation mechanism are suggested, and lessons learned are discussed. The significance of this study is to mitigate the catastrophic damage and failure caused by failure of GRS structures with marginal backfill during rainfall

2 CASE HISTORY

2.1 *Slope design and construction*

The multi-tier (GRS) slope investigated in this study was constructed 2010 to stabilize unstable slope on a road side that provided traffic access to a landfill in mountainous area in Dali District, Taichung County, Taiwan. As shown in Figure 1, wrap-around geogrid reinforcements with sandbag at front and rear were used. Locally available, low draining soil (with 60% fines) from weathered sandstone was used as backfill material (Figure 1). This could have been as a result of attempting to reduce cost and environmental impact associated with transportation of recommended backfills to construction site and disposal of excavated in-situ soils. A scrutiny of the original design revealed that as proposed by design guidelines limit equilibrium analysis (LE) was carried to check both the internal and external stability of the GRS slope. During design, phreatic surface was assumed to be at the middle between retained weathered layer and the slope surface and no attention was paid to soil hydraulic conductivity.

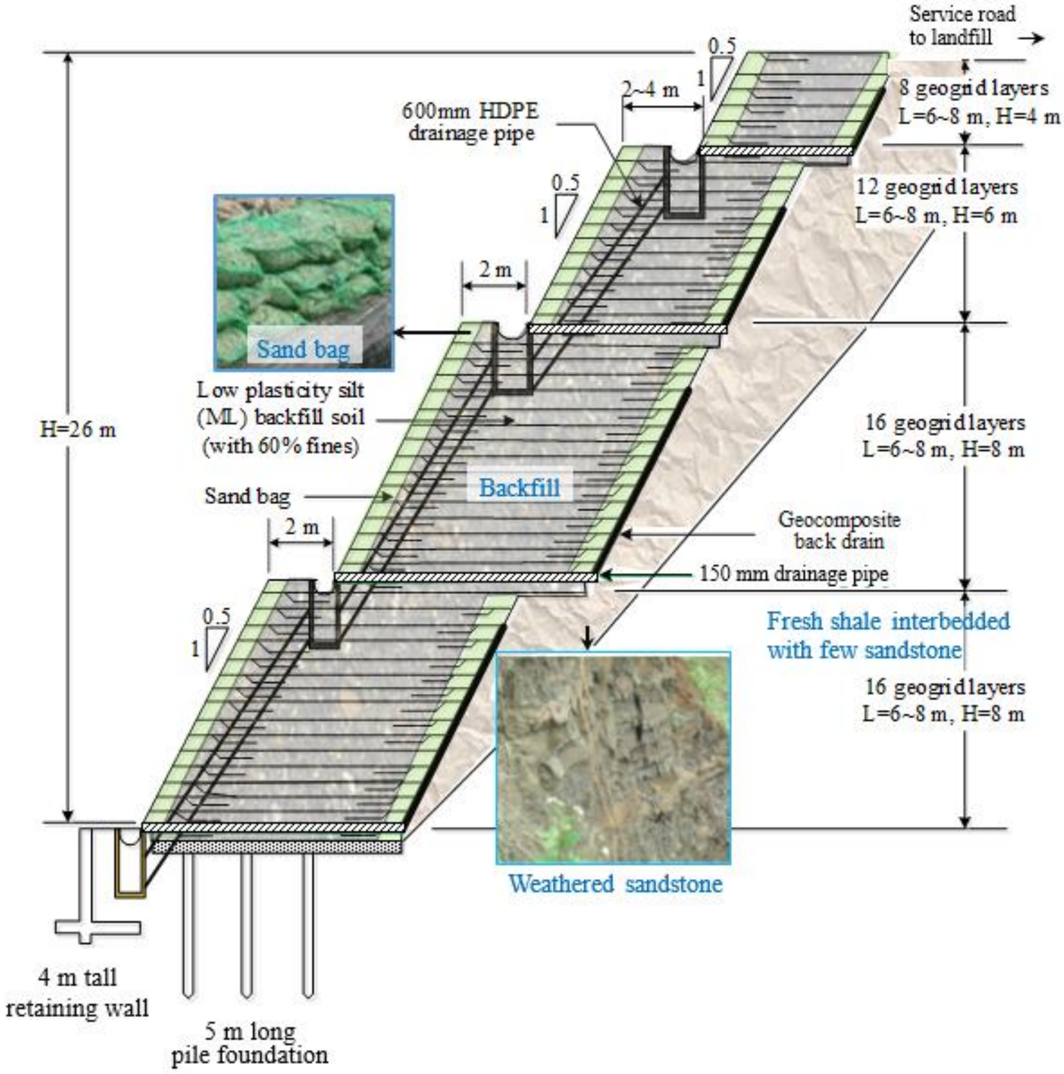

Figure 1 Layout and design details of multi-tier geosynthetics-reinforced soil slope

The slope construction process consisted of placing reinforcement, the front and rear sand bags, placing of backfill, backfill compaction process, and wrap around at the front and the rear side. Geocomposite back drains were place at the back slope and connected to 150 mm transverse drain pipes which were laid at a spacing of 2 m at the bottom of each tier. The 150 mm transverse drainage pipes were perforated on the upper surface to allow seeping out of accumulated water from the backfill soil into the pipe. To prevent soil particles from getting into the pipe, nonwoven geotextile was used to wrap the transverse drains. However, no filtration check to prevent clogging of nonwoven geotextile was reported. The 300 mm surface drains were provided at the slope surface to guide the collected water to an open drain at the bottom of each tier. Figure 2 shows the drainage joint connection details were poorly done and attention was not paid for easy of getting disconnected during settlement.

(a)

(b)

Figure 2. Drainage installations: (a) connection joint between back drain and transverse pipe; (b) connection joint between drainage ditch and vertical pipe (from Taiwan Professional Geotechnical Engineers Association report, 2014)

2.2 *Slope history and monitoring*

The slope was subjected to a series of wetting and drying seasons during its service life. Much of the rainfall was concentrated within a total of six major typhoons. Two months prior to completion of the construction process (July 2010), a tension crack was formed at the crest of the slope within the retained weathered sandstone layer. Thereafter, crack development continued followed by slope settlement. Typhoon Fanapi on September 2010 however induced excessive settlement (over 1 m) on top of the slope. From January to April 2010, the slope was repaired by means of placing additional 1 m high of extra backfill material on the top of the 3rd and 4th tier to cover for the settlement that had happened.

However, after typhoon Muifa on August 2011, crack development and settlement continued. With intention of designing for the remedial measures, slope deformation was monitored for a period of 7 months between June and December 2012. Deformation monitoring was done by means of recording relative heights of three established points on the top of 3rd and 4th tier using a dumpy level machine. Figure 3 shows recorded settlement of the top tier during this period. During this duration, the slope was subjected to two major typhoons, typhoon Talim (cumulative precipitation, R =350 mm) and Tyhoon Saola (cumulative precipitation, R = 563 mm). It was observed that after seasons of heavy rainfall (typhoon), considerably settlement of the top tier was observed (Figure 3)

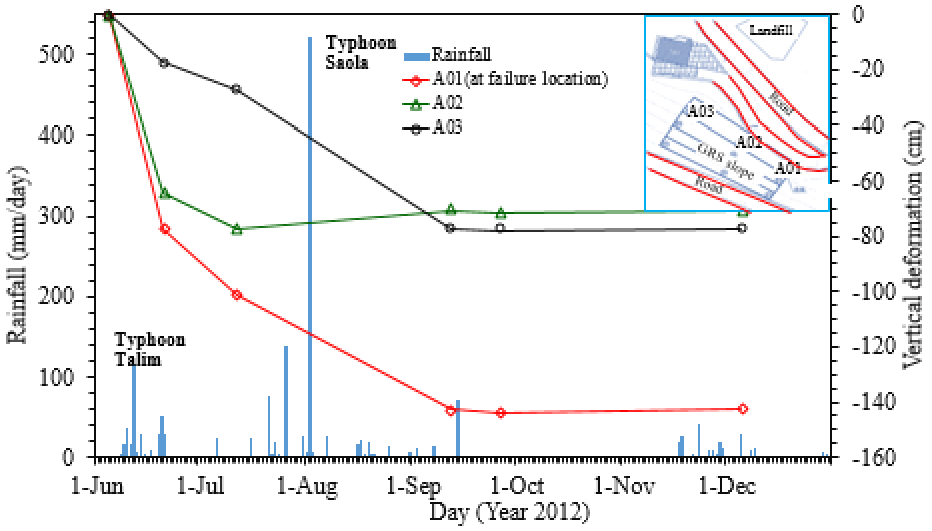

Figure 3. Relationships between rainfall and slope settlement

2.3 *Slope failure*

The slope final collapse happened on September 1, 2013, (Figure 4) exactly three years after completion. The collapse was preceded by two consecutive typhoon events, typhoon Trami (cumulative precipitation, R = 338 mm) and typhoon Kong-rey (cumulative precipitation, R = 310 mm) bringing a total precipitation of 647 mm. A few hours after the slope failure, ground water seeped out of the backfill soil and ponded at the slope toe (Figure 4). This suggested that pore water brought about by typhoon may have accumulated within the backfill soil.

From the preliminary investigations, causes of wall failure are:

i. The use of marginal soil (over 60% of fines) as backfill contrary to the backfill recommendations in design guidelines. Porewater pressure developed within the poorly draining backfill soils
ii. The original design and site investigation overlooked the existence of retained weathered rock layer, which has shear strength properties less than that of intact rock.
iii. Settlement and tension crack at the slope top surface allows rain water ponding at the slope top surface and consequently infiltrating into reinforced zone.
iv. Drainage system malfunctioned because drainage joints were poorly connected during construction and likely dislocated due to excessive slope deformation.
v. The soil fine particles may have clogged the nonwoven geotextile filter and hence retarded the drainage capacity.

In order to evaluate the effect of poor backfill hydraulic conductivity to slope settlement and eventual failure, coupled hydro-mechanical analysis was performed

(a)

(b)

Figure 4. Slope failure: (a) slope toe with water seeping out from backfill; (b) another view at the slope toe with-water ponding (from Taiwan Professional Geotechnical Engineers Association report, 2014)

3 NUMERICAL SIMULATION

3.1 *Numerical model and boundary conditions*

GRS slope two-dimensional FE model is displayed in Figure 5. The slope geometry was constructed according to topographic maps and the subsurface soil profiles were interpolated from the borehole logging readings. The numerical model consists of a total of 3195 fifteen-node triangular elements. Fine-element meshes were specified for the backfill and weathered soil layers whereas medium-element meshes were applied to rock layers (Figure 5). Standard fixity was applied as the mechanical boundary; the two lateral boundaries were allowed to move only in the vertical directions whereas the bottom boundary was restrained from movement.

Hydraulic boundaries at two lateral ends were initially set to be constant head boundary conditions on the basis of the assumed ground water table (GWT) levels. During the analysis, the hydraulic boundaries were switched to seepage boundary conditions to enable variations in GWT levels because of wetting and drying cycles. Downward vertical influx was prescribed on the slope surface to model rainfall, whereas upward influx was imposed on the surface boundary to simulate evapotranspiration. The input values of downward flux during rainfall were obtained from the actual rainfall records from the nearest precipitation measuring station. The value of upward flux on dry days was estimated to be 10 mm/day based on studies on the average evapotranspiration rate of mountain areas in Taiwan

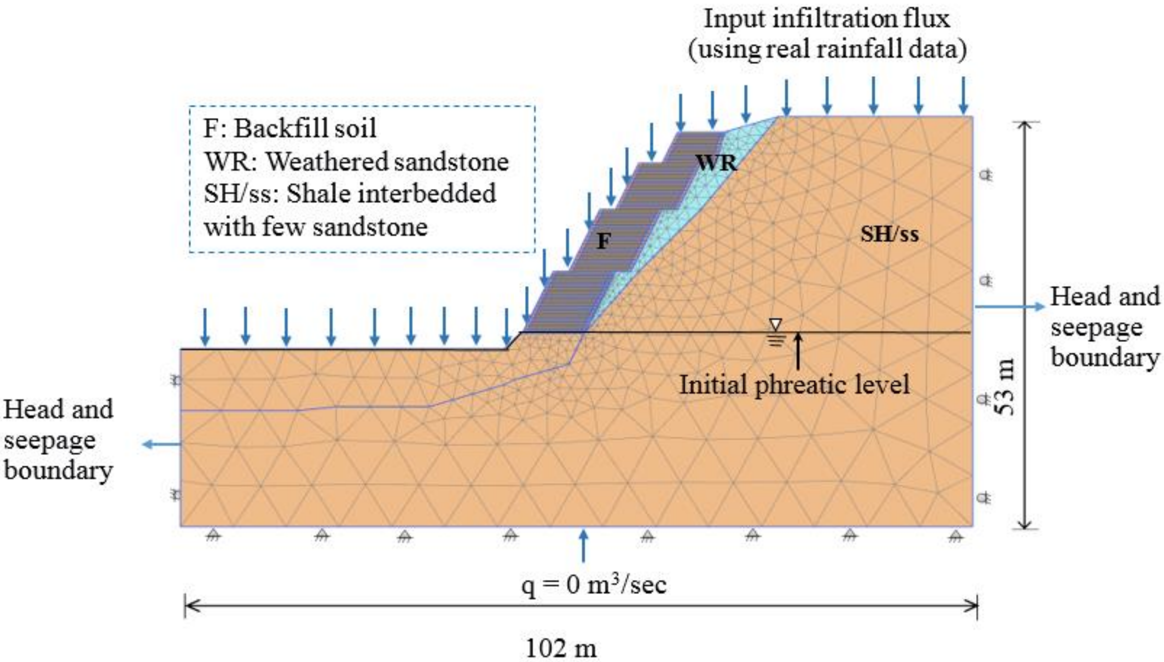

Figure 5. Numerical mesh and boundary conditions

3.2 *Material properties*

Table 1 is a summary of material properties. Backfill soil was modeled as a stress-dependent, hyperbolic, elastoplastic material by using the Hardening Soil model and was analyzed using effective stress parameters under drained conditions. Weathered sandstone, shale and sand were modelled using Mohr Coulomb model. Material hydraulic are summarized in Table 2.

Table 1. Material properties

Soil/rock layer	Analysis type	Saturated unit weight, γ_{sat} (kN/m^3)	Poisson ratio, ν', ν_u	Cohesion, c', $q_u/2$ (kPa)	Friction angle, ϕ', ϕ (°)	Young's Modulus E, E_u, (kPa)
Backfill (F)	Unsaturated Drained	21	0.3	23, 6	37,37	$E_{50}^{ref} = 29500$
Weathered sandstone (WR)	Unsaturated Drained	23	0.3	2.7, 1.4	33, 31	1.16×10^5
Shale (SH/ss)	Saturated Undrained	22	0.495	1500	0	1.5×10^6
Sand (S)	Saturated Drained	17	0.3	5	39	4.76×10^5

Note: shear strength properties of backfill soil and weather layer are for peak and residual shear strength, respectively.

Table 2. Material hydraulic properties

Parameter	Backfill (F)	Weathered Sandstone (WR)		Shale (SH/ss)	Sand (S)
k_s, Saturated hydraulic conductivity (m/s)	1×10^{-7}	1×10^{-6}		1×10^{-10}	1.35×10^{-4}
θ_s, Saturated volumetric water content, (%)	32.7	32.4	21	-	-
θ_r, Residual volumetric water content, (%)	10	21	0.02	-	-
n, van Genuchten model fitting parameter	1.78	2.8	2.8	-	-
α, van Genuchten model fitting parameter (kPa^{-1})	0.106	0.1	3.33×10^{-3}	-	-

Geogrid specimen was retrieved from failed slope in the field and tested by Single Rib Tensile Method to determine it long-term tensile strength. Test results indicate the long-term tensile strength of the retrieved geogrid $T_{ult\ (retrieved)}$ =113 kN/m.

3.3 *Initial conditions*

Upon simulating the wall construction, the initial PWP was generated by prescribing a specified flux at the top of the slope model for a considerable time until steady state conditions were reached. The quantities of the prescribed flux were first adjusted until the calculated initial matric suction value fell within the range of expected field suctions. Considering that during the construction of earth-retaining structures in the field, backfill soils are compacted at ±2% of the optimum moisture content, target suction of 40 kPa was obtained from the backfill SWCC corresponding to optimum moisture content of 11.8 % obtained during standard proctor test. In addition, a pre-rainfall period of 20 days was simulated using the actual rainfall data from July 1 up to July 20, 2013 in order to establish initial hydrology conditions.

4 RESULTS AND DISCUSSION

Fully coupled flow deformation module was implemented into the PLAXIS (version 2D 2015) finite element (FE) program (Brinkgreve et al., 2016). Figure 6 shows model validation results for the failure of GRS slope in 2013 by comparing the predicted and observed failure timing. The FS of the slope dropped at each rainfall event and recovered during dry days because of the effect of modeling evapotranspiration. It is observed that the predicted failure timing (FS=1) using residual soil shear strength corresponds with the observed failure timing. Slope had undergone excessive deformation before failure hence shear strength properties at failure were considered to be residual properties. This indicates that the developed hydro-mechanical model is capable of accurately predicting the timing of rainfall-induced slope failure.

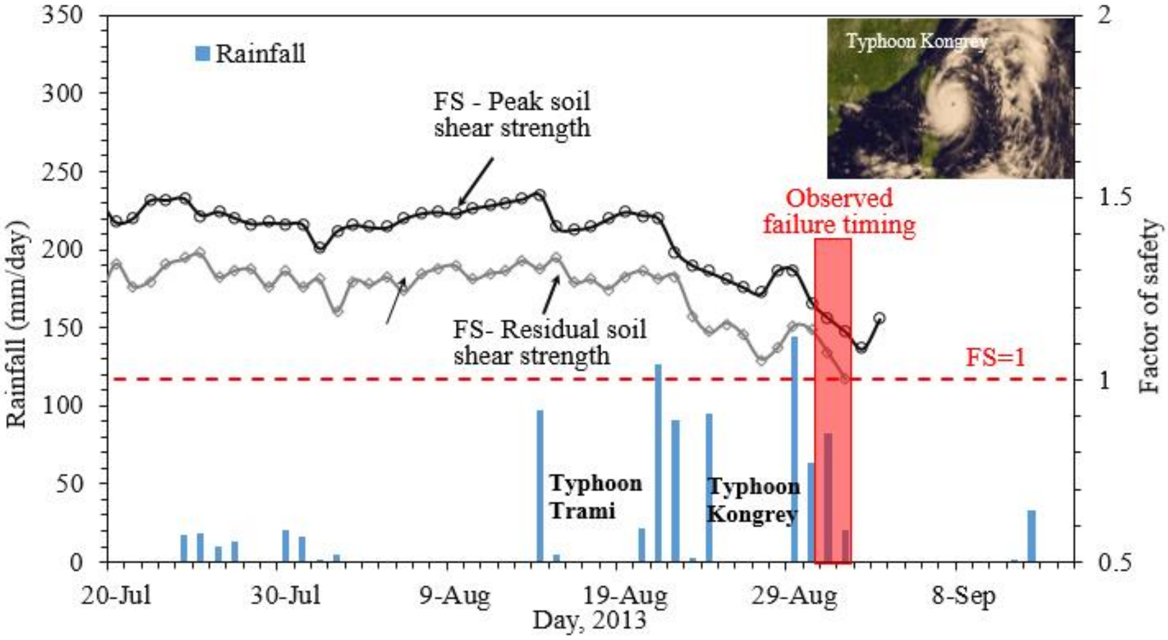

Figure 6. Predicted factor of safety variation results.

Predicted deformed mesh at failure is shown in Figure 7. The deformed mesh shows that large deformations occurred in both the backfill soil and the weathered sandstone layer. The failure surface partially cuts through the bottom tier of the GRS slope and partially passes through the weathered sandstone (Figure 8). This suggests compound failure mode occurred within the slope. Weathered sandstone layer, though overlooked in the initial reinforced slope design may have been unstable and contributed to slope failure. The predicted deformed shape imitates the shape of the failure mass observed after slope failure (Figure 4).

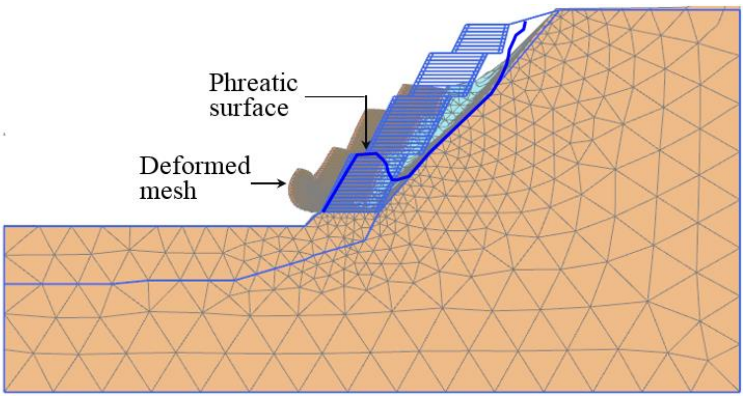

Figure 7. Deformed mesh and phreatic surface at slope failure

From Figure 7, it is also observed that the GWL had risen to the top of the bottom tier. The bottom tier is fully submerged. This is contrary to the initial design assumption where GWL was assumed to be at the middle of the backfill soil (between retained fill and ground surface). Therefore, slope failure was attributed to the increase of PWP (loss of soil matric suction) due to the rise of phreatic surface level.

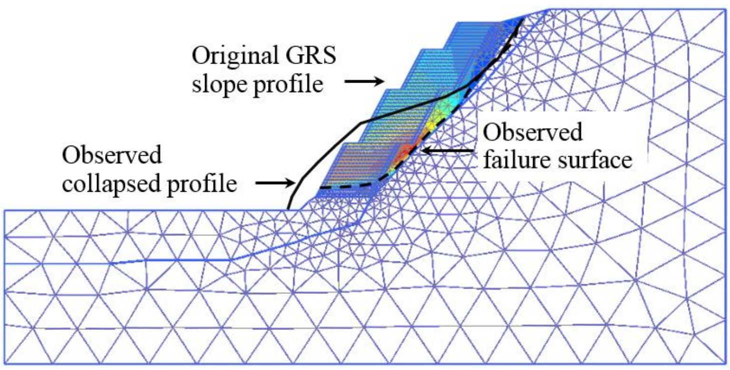

Figure 8. Incremental displacements contours at slope failure and compared with observed failure plane surface

5 LESSONS LEARNED AND SUGGESTED REMEDIAL MEASURES

From the discussed failure investigation and couple hydromechanical analysis, the following lessons were learned and remedial measures were suggested:

a) The use of marginal soil as backfill compromised the performance of the GRS slopes upon rainfall infiltration because its low draining capacity could cause the build-up of PWP, and finally lead to the slope failure.
b) The original site investigation failed to identify the existence of the weak soil layer (weathered rock layer). More detailed site investigation is required during design of GRS structures
c) Because of the compound failure mode, it is crucial to stabilize unstable weathered rock prior to the construction of the GRS slope in front of it.
d) Because high positive pore water pressures accumulated at the slope toe, sufficient drainage should be provided, especially at the bottom tier of the GRS slope.
e) The rear sand bags which show daylight at the top of the slope could provide a flow channel to facilitate rainfall infiltration. It is suggested that rear sand bags should not show daylight.
f) Filter criteria should be checked for nonwoven geotextile used to wrap drainage pipes or in geocomposite to avoid clogging of geotextile by fine soil particles.
g) Excessive deformation of marginal soil could occur upon rainfall infiltration. Hence flexible drainage joints should be used to avoid drainage joints disconnection caused by slope deformation.

6 CONCLUSIONS

From the findings of this study, the following conclusions were made:

i. This study demonstrated that using recorded rainfall, measured soil parameters, site geology and slope geometry, the hydro-mechanical model based on the framework of unsaturated soil mechanics is capable of accurately predicting the failure timing of a GRS slope.
ii. The slope failure was attributed to increase of pore water pressure (loss of matric suction). The phreatic surface level advanced to the weathered rock and increase to the top of the bottom tier of the GRS slope.
iii. Efficient and sufficient drainage systems are required to improve system drainage capacity and hence enhance the system stability during rainfall.

For the purpose of effective risk management, coupled hydro-mechanical analyses combined with detailed site investigation could be performed to establish the FS vs. accumulated rainfall relationship for slopes which could affect major protected properties or residents. The results of the analyses provide a valuable reference for identifying and assessing potential hazardous sources to subsequently formulate disaster prevention and mitigation strategies (e.g., establishing early warning systems and evacuation plans or applying engineering approaches to enhance slope stability to reduce rainfall infiltration)

REFERENCES

AASHTO, 2002. Standard Specifications for Highway Bridges. , Seventeeth ed. American Association of State Highway and Transportation Officials, Washington, D.C., with interims.

Brinkgreve, R.B.J., Kumarswamy, S., Swolfs, W.M., 2016. PLAXIS 2016 Manual, Balkema, Rotterdam, The Netherlands.

Christopher, B.R., Stulgis, R.P., 2005. Low permeable backfill soils in geosynthetics reinforced soil wall: state of the practice in North America., Proceedings of North American GeosyntheticsConference (NAGS 2005), , Las Vegas, NV, USA, GRI-19, p. p. 14e16.

Elias, V., Christopher, B.R., and Berg, R., 2001. Mechanically stabilized earth walls and reinforced soil slopes design and construction guidelines. Report No. FHWA-NHI-00-043, National Highway Institute, Federal Highway Administration, Washington, D.C. March.

Hamdhan, I.N., Schweiger, H.F., 2013. Finite Element Method–Based Analysis of an Unsaturated Soil Slope Subjected to Rainfall Infiltration. International Journal of Geo-mechanics of Materials 13, 653-658.

Hedayati, M., Hossain, S., 2015. Data based model to estimate subgrade moisture variation case study: Low volume pavement in North Texas. Transportation Geotechnics 3, 48-57.

Koerner, R., koerner, G., 2012. A Data Base and Analysis of 141 Geosynthetic Reinforced Mechanically Stabilized Earth (MSE) Walls, 226th Pennsylvania Geotechnical Conference Hershey, PA.

Ku, C.-Y., Hsu, S.-M., Chiou, L.-B., Lin, G.-F., 2009. An empirical model for estimating hydraulic conductivity of highly disturbed clastic sedimentary rocks in Taiwan. Engineering Geology 109, 213-223.
Leshchinsky, D., 2009. On Global Equilibrium in Design of Geosynthetic Reinforced Walls. Journal of Geotechnical and Geoenvironmental Engineering 135, 309-315.
Mitchell, J.K., Zornberg, J.G., 1995. Reinforced soil structures with poorly draining backfills. Part II: case histories and applications. . Geosynthetics International 2, 265-307.
Oh, S., Lu, N., 2015. Slope stability analysis under unsaturated conditions: Case studies of rainfall-induced failure of cut slopes. Engineering Geology 184, 96–103.
Portelinha, F.H.M., Bueno, B.S., Zornberg, J.G., 2013. Performance of nonwoven geotextile-reinforced walls under wetting conditions: laboratory and field investigations. Geosynthetics International 20, 90-104.
Qi, S., Vanapalli, S.K., 2015. Hydro-mechanical coupling effect on surficial layer stability of unsaturated expansive soil slopes. Computers and Geotechnics 70, 68–82.
Thuo, J.N., K.H.Yang, Huang, C.C., 2015. Infiltration into unsaturated reinforced slopes with nonwoven geotextile drains sandwiched in sand layers. Geosynthetics International 22, 457–474.
Vahedifard, F., Mortezaei, K., Leshchinsky, B.A., Leshchinsky, D., Lu, N., 2016. Role of suction stress on service state behavior of geosynthetic-reinforced soil structures. Transportation Geotechnics.
Yang, K.-H., Uzuoka, R., Thuo, J.N., Lin, G.-L., Nakai, Y., 2017. Coupled hydro-mechanical analysis of two unstable unsaturated slopes subject to rainfall infiltration. Engineering Geology 216, 13-30.
Zornberg, J.G., Mitchell, J.K., 1994. Reinforced Soil Structures with Poorly Draining Backfills. Part I:Reinforcement Interactions and Functions. Geosynthetics International 1,No. 2, 103-148.